Magnetic and electronic properties of $Bi_{0.75}Ca_{0.25}MnO_3$

2007 J. Phys.: Condens. Matter 19 406212

(http://iopscience.iop.org/0953-8984/19/40/406212)

J. Phys.: Condens. Matter **19** (2007) 406212 (9pp) doi:10.1088/0953-8984/19/40/406212

Magnetic and electronic properties of $Bi_{0.75}Ca_{0.25}MnO_3$

J L García-Muñoz[1], C Frontera[1], P Beran[1], N Bellido[2], J S Lord[3], C Ritter[4] and I Margiolaki[5]

[1] Institut de Ciència de Materials de Barcelona, CSIC, Campus Universitari de Bellaterra, E-08193 Bellaterra, Spain
[2] Laboratoire CRISMAT, UMR 6508 CNRS/Ensicaen, 6 boulevard du Maréchal Juin, F-14050 Caen Cedex, France
[3] ISIS Facility, Rutherford Appleton Laboratory, Chilton, Oxon OX11 0QX, UK
[4] Institut Laue Langevin, BP 156, F-38042 Grenoble Cedex 9, France
[5] European Synchrotron Radiation Facility, ESRF, BP 220, F-38043 Grenoble, France

Received 30 May 2007, in final form 12 July 2007
Published 12 September 2007
Online at stacks.iop.org/JPhysCM/19/406212

Abstract

The magnetic, structural and electronic properties of $Bi_{0.75}Ca_{0.25}MnO_3$ have been investigated in comparison with those of $Bi_{0.75}Sr_{0.25}MnO_3$. Magnetometry, diffraction and muon spin relaxation (μSR) data confirm different structural, magnetic and electronic transitions in the two compounds. The anisotropic changes of cell parameters across the structural transition in $Bi_{0.75}Ca_{0.25}MnO_3$ (275 K) differ markedly from the lattice anomalies in $Bi_{0.75}Sr_{0.25}MnO_3$ (600 K) and also from those in $Bi_{0.50}Ca_{0.50}MnO_3$ (325 K). The ground state of $Bi_{0.75}Ca_{0.25}MnO_3$ is characterized by a high degree of spin disorder and frustrated interactions. There is no evidence of a ferromagnetic component in the ground state of $Bi_{0.75}Ca_{0.25}MnO_3$. However, the application of a magnetic field (even of a few gauss) produces a continuous progressive polarization of the Mn moments ($\approx 2\ \mu_B$/Mn at 5 T, ZFC, 5 K). Differences between Ca and Sr perovskites with $x = 1/4$ are greater than for the $x = 1/2$ counterparts, and point to distinct ground states and charge/orbital configurations.

1. Introduction

In mixed-valence metal oxides the electronic-type transitions related with charge localization, orbital ordering (OO) assisted by the Jahn–Teller effect, and charge ordering (CO) are currently the object of intense investigations. The Bi–Sr–Mn–O system is receiving great attention due to the observation of some singularities that differ from the general behaviour of previously studied manganites. One of the most remarkable differences is the great tendency of Bi–Sr manganites to present charge/orbital order (COO) at very high temperatures [1–10]. An unexpected discovery was that charge order is much more favoured in (Bi, Sr)MnO_3 than in

(Bi, Ca)MnO_3 manganites. So, despite Ca being clearly smaller than Sr, the melting of the charge-ordered phase occurs at $T_{CO} \approx 325$ K in $Bi_{0.50}Ca_{0.50}MnO_3$ and at $T_{CO} \approx 525$ K in $Bi_{0.50}Sr_{0.50}MnO_3$ [1, 2]. Moreover, high-resolution electron microscopy studies have revealed a distinctive contrast modulation (with the periodicity of alternating double rows of octahedra) in distinct charge-ordered phases of $Bi_{1-x}Sr_xMnO_3$ compounds ($x = 0.5, 0.25, \ldots$), not observed in $Bi_{1-x}Ca_xMnO_3$ [3, 6].

The composition $Bi_{0.75}A_{0.25}MnO_3$ (A = Ca and Sr) is particularly appealing due to its commensurability ($x = 1/4$). So, we have recently established the existence of a new type of charge-ordered phase in $Bi_{0.75}Sr_{0.25}MnO_3$ [5, 7, 9], the only known $Ln_{0.75}A_{0.25}MnO_3$ manganite presenting COO. $Bi_{0.75}Sr_{0.25}MnO_3$ undergoes a charge-order transition at $T_{CO} = 600$ K, well above the ordering temperature in half-doped $Bi_{0.5}Sr_{0.5}MnO_3$ ($T_{CO} = 525$ K), giving a superstructure that doubles two of the pristine cell parameters. This also strongly contrasts with the behaviour of other manganites, where $x = 0.5$ presents the optimal temperature for CO, and $x < 0.5$ compositions present the same superstructure as the $x = 0.5$ case.

$BiMnO_3$, a ferromagnetic insulator ($T_C = 105$ K), crystallizes at high pressure in a highly distorted perovskite structure. The lone pair of Bi drives the off-centre distortion in $BiMnO_3$, producing its multiferroic behaviour [11]. $BiMnO_3$ is a prototypical magnetic ferroelectric, with a Curie temperature of around 770 K, remaining ferroelectric down to low temperatures through the ferromagnetic transition at 105 K [12, 13]. It is thus one of the very few monophasic materials exhibiting biferroicity, although the origin of the ferromagnetism in pure $BiMnO_3$ is not yet well understood. Moreover, the dependence of the properties of $Bi_{1-x}Sr_xMnO_3$ compounds on the Sr content is still an open issue. Chiba *et al* found that doping with Sr systematically decreases the ferromagnetic moment from the saturation value of 3.6 μ_B observed in the parent $BiMnO_3$ perovskite. The ferromagnetic component only disappeared at doping levels $x > 0.4$ [14]. Recently, by using neutron powder diffraction, we have determined that the ground state for $x = 0.25$ is antiferromagnetic and that the magnetic moment found in magnetization measurements is due to the magnetic field applied for the magnetization measurements. It is of great interest to investigate the low doping regime of $Bi_{1-x}A_xMnO_3$ (A = Ca, Sr), among others, for the following two reasons. The first is to characterize how the large differences found at the $x = 0.5$ level behave in the low doping region. The second is to study how these systems recover the biferroicity of the parent $BiMnO_3$ compound. In this work, we present a study on the properties of $Bi_{3/4}Ca_{1/4}MnO_3$, in comparison with those of the Sr analogue. Our results suggest a new ground state due to a distinct charge/orbital configuration.

2. Experimental details

Two polycrystalline samples of $Bi_{3/4}Ca_{1/4}MnO_3$ and $Bi_{3/4}Sr_{1/4}MnO_3$ were prepared following a sol–gel route, starting from stoichiometric quantities of Bi_2O_3 (99.9%), MnO_2 (99.99%), and $SrCO_3$ or $CaCO_3$ (99.99%). Sol–gel synthesis was chosen with the purpose of obtaining a single-phase material at relatively low temperature to minimize a possible Bi deficiency due to evaporation. A detailed description of sample preparation and preliminary characterization has been previously reported in [7, 9, 15].

Structural studies were done by means of synchrotron x-ray powder diffraction (SXRPD) and neutron powder diffraction (NPD). SXRPD data were collected at the ID31 beamline of ESRF (Grenoble, France), and NPD data at D1B and D2B diffractometers of ILL (Grenoble, France).

Muon spin relaxation (μSR) measurements were conducted at the ISIS pulsed muon facility (Rutherford Appleton Laboratory, Chilton, UK) using the EMU instrument. μSR provided additional information on the magnetic homogeneity/inhomogeneity in these oxides.

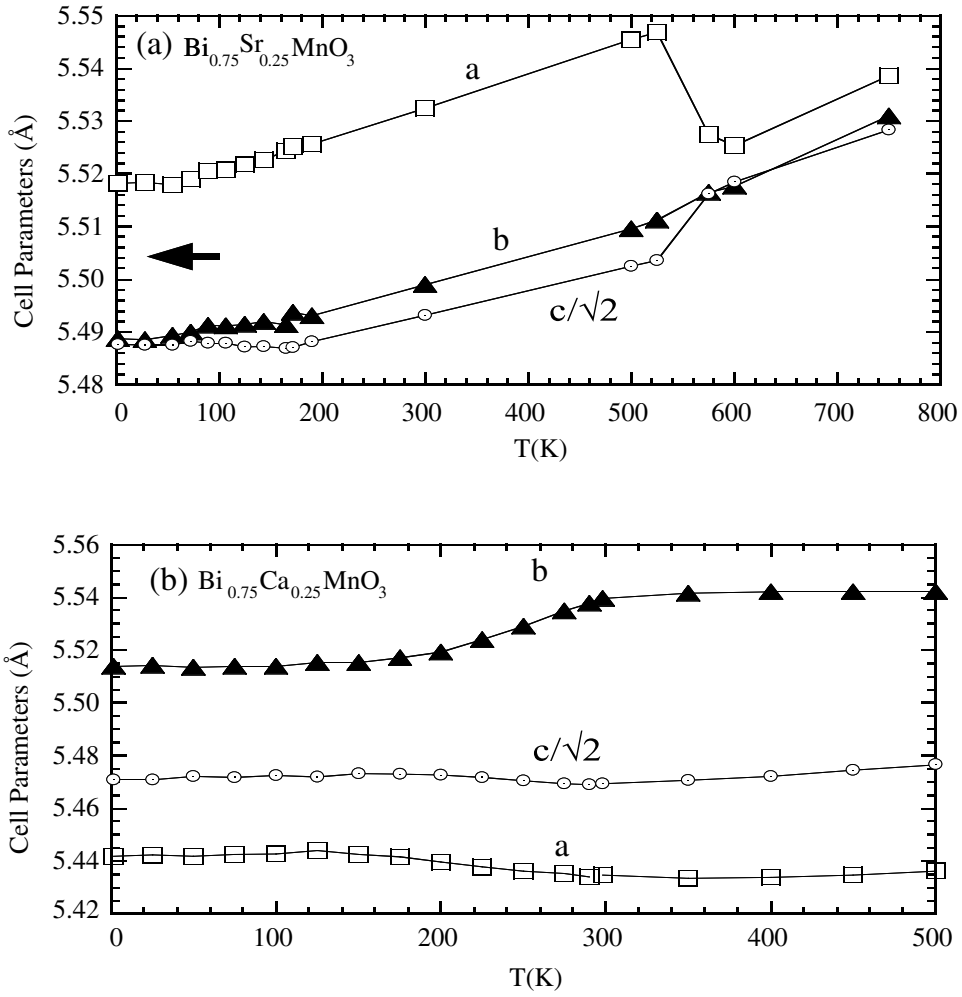

Figure 1. Temperature dependence of the lattice parameters across the structural and electronic transitions: (a) $Bi_{0.75}Sr_{0.25}MnO_3$, (b) $Bi_{0.75}Ca_{0.25}MnO_3$.

The two polycrystalline samples were investigated in longitudinal geometry below room temperature (RT) using a closed-cycle refrigerator (5 K $\leqslant T \leqslant$ 300 K). Fully polarized positive muons were implanted in the sample. The subsequent evolution of muon polarization occurs in response to the coupling between the muon spin and the internal magnetic fields. The decay of the muon ($\tau_\mu = 2.2\ \mu$s) is accompanied by positron emission preferentially along the muon spin direction. This permits monitoring the evolution of the implanted muon polarization through the relaxation function $G_z(t) = a_0 P(t)$, where a_0 is the initial asymmetry.

3. Results and discussion

3.1. Neutron and synchrotron diffraction

Neutron (D1B and D2B, ILL) and synchrotron (ID31, ESRF) diffraction data confirmed a different ground state in these compounds with $x = 1/4$. In figure 1 we have represented the evolution of the lattice parameters in a wide temperature range down to 2 K. It is apparent

in figures 1(a) and (b) that the two compounds undergo different structural transitions at, respectively, 275 K (Ca) and 625 K (Sr). Moreover, the qualitative differences in the anomalies observed confirm that the two structural changes are different, and point to two distinct ground states and charge/orbital configurations at low temperatures in the case of Ca and Sr. The changes around 600 K shown in figure 1(a) were previously reported in [5, 7, 9]. According to our previous results, the anisotropic evolution of the lattice of the Sr compound (figure 1(a)) is caused by the entering on cooling of a charge-ordered state characterized by a double lattice modulation, ($\frac{1}{2}$ 0 0) and (0 0 $\frac{1}{2}$), on a $Ibmm$ subcell [7, 9]. Across the structural transition the average structure changes from $Ibmm$ below T_{CO} to $Pbnm$ above T_{CO} [6, 7, 16], a sudden symmetry change that is not common in modulated manganites.

An important result of the present study is the very different behaviour of $Bi_{3/4}Ca_{1/4}MnO_3$ (figure 1(b)). In contrast with the Sr-doped oxide, this Ca manganite exhibits a cell anomaly around 275 K. This anomaly is characterized by a slightly anisotropic evolution of lattice parameters, which experience the contraction (expansion) on cooling of b (a) lattice parameters, while c remains almost unchanged. At this point, it is of interest to emphasize that these changes are also different to those found in the half-doped Bi–Ca or Ln–Ca charge-ordered manganites (where a and b increase and c decreases [2]). Moreover, they also differ from changes reported for the $x \approx 1/3$ doping in rare-earth-based manganites (as, for instance, in $Pr_{0.67}Ca_{0.33}MnO_3$ [17]). On the other hand, the symmetry of the average cell with Ca is likely the same at both sides of the transition in figure 1(b), in contrast with the behaviour found for $Bi_{3/4}Sr_{1/4}MnO_3$. Across this transition, some new structural satellites appear on cooling in the SXRPD patterns. These satellites (appearing/disappearing at the transition) can be indexed by using the wave vectors ($\frac{1}{2}$ 0 0) and (0 0 $\frac{1}{2}$) referred to the $a_p\sqrt{2} \times a_p\sqrt{2} \times 2a_p$ cell as in the Sr compound, but they can also be indexed by adopting the monoclinic cell described by Atou *et al* for $BiMnO_3$ [18, 14]. It is worth mentioning that above this transition the structure also presents superstructure peaks. Many of them need a monoclinic $2a \times b \times 2c$ ($2a_p\sqrt{2} \times a_p\sqrt{2} \times 4a_p$) cell to be indexed, and cannot be indexed with the cell used by Atou *et al* or, equivalently, by Giod *et al* [18, 19] ($\sqrt{6}a_p \times \sqrt{6}a_p \times \sqrt{2}a_p$). But some others cannot be indexed with this supercell. We recall that a minor polymorphic phase was found to coexist with the monoclinic $C2$ phase in $BiMnO_3$ [20]. Further studies aimed at determining this supercell without ambiguity are currently in course.

In the inset of figure 2(b) we show the evolution of the low-angle portion of the neutron diffraction patterns ($\lambda = 2.52$ Å, D1B) of $Bi_{0.75}Ca_{0.25}MnO_3$. A remarkable result is the absence of apparent magnetic reflections at low temperatures. This is a relevant unexpected finding that confirms the absence of a well-developed long-range magnetic order in the Ca compound. A very weak residual signature of pseudo-CE order (see [1]) can still be appreciated with difficulty in NPD data (inset in figure 2(b)). Regarding the sample as magnetically homogeneous, this small signal would imply a very low average ordered moment of $0.5\mu_B$/Mn. The evolution of the Mn ordered moment in $Bi_{0.75}Ca_{0.25}MnO_3$ and $Bi_{0.75}Sr_{0.25}MnO_3$ is plotted in figure 3. Data for $Bi_{0.75}Sr_{0.25}MnO_3$ in this figure were obtained as explained in [9]: D1B neutron diffraction patterns collected as a function of temperature were fitted using the pseudo-CE magnetic structure reported in [9] for the same sample of $Bi_{0.75}Sr_{0.25}MnO_3$ (see also figure 6 in [9]).

$M(H)$ and $M(T)$ measurements are plotted in figure 2. The evolution of the magnetization $M(T)$ shows a weak ferromagnetic signal below ≈70 K, although the comparison of field-cooled (FC) and zero-field-cooled (ZFC) curves ($H = 1000$ G) is indicative of magnetic disorder, and a possible freezing around 30 K. The spin-glass-like behaviour detected below $T \approx 70$ K originates at the majority regions of the sample, and coexists with a very small residual phase showing extremely weak pseudo-CE-type magnetic order.

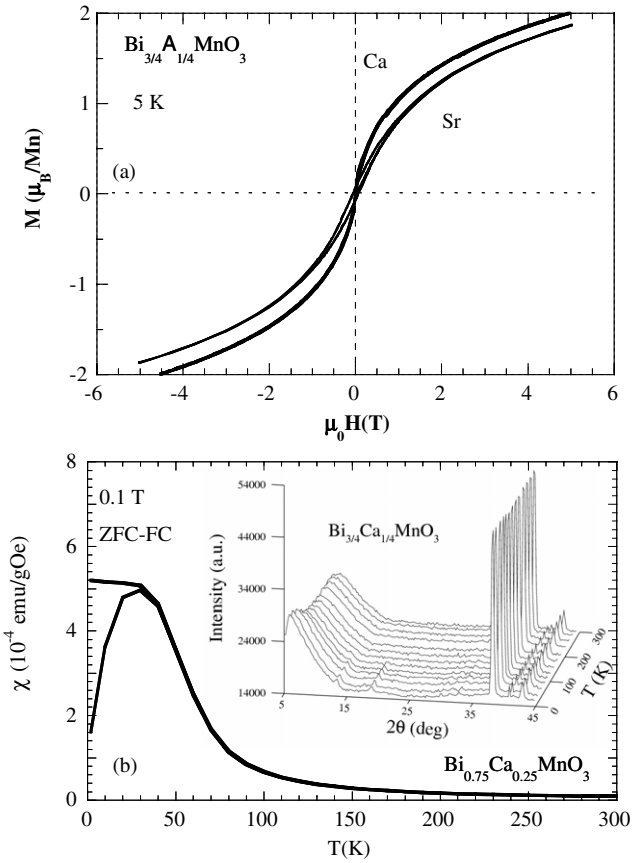

Figure 2. (a) $M(H)$ of $Bi_{0.75}A_{0.25}MnO_3$ (ZFC, 5 K) obtained during a hysteresis cycle (A = Ca and Sr). The small opening of the hysteresis cycle of $Bi_{0.75}Sr_{0.25}MnO_3$ (with coercive field of 0.06 T and a remanence magnetization of 0.07 mB/Mn) is due to an small amount of hausmannite (2% as reported in [6]) that is ferrimagnetic below (T_C = 47.5 K). (b) FC–ZFC susceptibility of $Bi_{0.75}Ca_{0.25}MnO_3$ (DC susceptibility measured under $\mu_0 H$ = 0.1 T). Inset: evolution in the temperature range 1.5–300 K of the low-angle portion of the neutron diffraction patterns (λ = 2.52 Å) of $Bi_{0.75}Ca_{0.25}MnO_3$ showing the practical absence of long-range magnetic order (a very weak residual signature of the $(\frac{1}{2}\ \frac{1}{2}\ 0)$ magnetic reflection can be appreciated at $2\theta \approx 18°$).

The coexistence of ferromagnetism and charge/orbital order under field in $Bi_{0.75}Sr_{0.25}MnO_3$ was reported and discussed in [7]. We found that the magnetic structure of $Bi_{0.75}Sr_{0.25}MnO_3$ in zero field is antiferromagnetic, with null ferromagnetic component, ruling out previous suggestions of intrinsic spontaneous ferromagnetism. This is corroborated by the $M(H)$ measurements shown in figure 2(a). This figure illustrates the field-dependent magnetization of the COO phase of $Bi_{0.75}Ca_{0.25}MnO_3$ and $Bi_{0.75}Sr_{0.25}MnO_3$ during a hysteresis cycle at 5 K (up to 5 T). Both display a similar field dependence. The $M(H)$ isotherms for $Bi_{0.75}Sr_{0.25}MnO_3$ and $Bi_{0.75}Ca_{0.25}MnO_3$ show an apparent nonlinear increase. The marked curvature confirms the induction of ferromagnetism by the external field. The ferromagnetic component increases continuously with the field, indicating a continuous progressive polarization of the Mn moments. Polarization is already visible, even for very small fields. Moreover, in the Ca perovskite the polarization is larger than in the Sr sample. We recall that, as for the gradual polarization in $Bi_{0.75}Sr_{0.25}MnO_3$, it has been suggested that the field-induced antiferromagnetic (AFM) to fer-

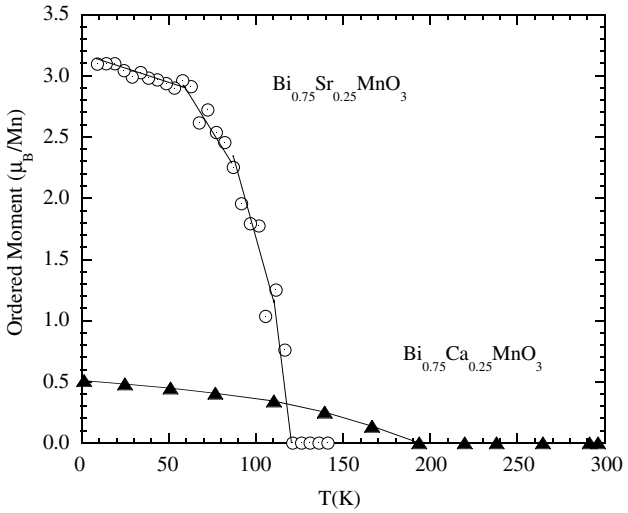

Figure 3. Dependence of the ordered magnetic moment per Mn ion determined from neutron data. The figure illustrates the extremely low value of the ordered moment in $Bi_{0.75}Ca_{0.25}MnO_3$.

romagnetic (FM) transition in $Bi_{0.50}Sr_{0.50}MnO_3$ is not accompanied by COO melting [21], in contrast with other manganites with no Bi [22].

3.2. μSR

In order to get additional information on the magnetic homogeneity/inhomogeneity in the ground state, both compositions were also characterized by μSR. The sample was mounted on an Al plate with a silver mask in a closed-cycle refrigerator.

Below RT, muon decay in $Bi_{3/4}Sr_{1/4}MnO_3$ is well reproduced using a single exponential ($G_z(t) = A\exp[(-(\lambda t)])$. The thermal evolution of the exponential relaxation rate (λ) and initial asymmetry is plotted in figure 4(a). The value of λ is, for all the studied temperature range, below (or around) 0.1 μs^{-1}. Such small values are typical of AFM correlations in manganites. The initial asymmetry drops slowly below $\approx$135 K, coinciding with the apparition of an ordered magnetic moment at Néel transition as found by NPD.

The behaviour is quite different in $Bi_{3/4}Ca_{1/4}MnO_3$. Muon depolarization adopts the stretched exponential form $G_z(t) = A_s\exp[(-(\lambda_s t)^{\beta})]$, more characteristic of inhomogeneous magnetic systems and spin-glasses (figure 4(b)). Concerning the initial asymmetry, a magnetic transition takes place at $T \approx 75$ K, producing a pronounced diminution of the initial asymmetry to a 70% of its initial value. Moreover, figure 4(b) also shows that there is a tiny, subtle deviation of the asymmetry from 1 below $T \approx 150$ K. This subtle decrease coincides with the apparition of a small ordered magnetic moment evidenced by NPD. This subtle deviation coincides with the drop of the exponent β that also deviates from 1 (inset of figure 4(b)). This drop signals the appearance of inhomogeneous magnetism in this compound.

In figure 5 we have plotted the temperature dependence of the relative fraction of muons feeling a local static field at their site. This fraction, obtained from the evolution of the initial asymmetry, is related to the relative volume fraction exhibiting some degree of magnetic order. Because of the pulsed structure of the ISIS beam, the rotation frequency of the muon spin induced by local magnetic order perpendicular to its polarization falls beyond the accessible frequency window at ISIS. Hence local magnetic order is seen as a loss of initial asymmetry

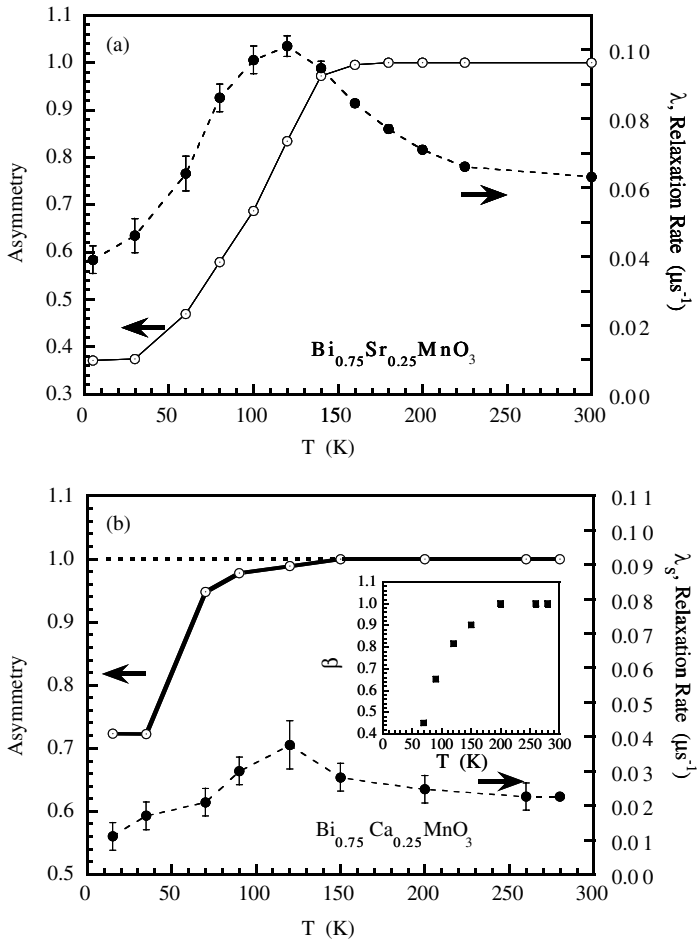

Figure 4. Temperature dependence of the initial asymmetry (normalized, left axis) and relaxation rate (right axis). (a) $Bi_{3/4}Sr_{1/4}MnO_3$ with λ: exponential relaxation rate. (b) $Bi_{3/4}Ca_{1/4}MnO_3$, λ_S: stretched exponential relaxation rate. The exponent β is shown in the inset.

(2/3 of the total asymmetry is lost in polycrystalline samples with magnetic order in the entire volume).

Some important conclusions can be extracted from this figure. The behaviour of Bi–Sr sample reflects the usual appearance of magnetic long-range order at $T_N \approx 120$ K in the whole system, as evidenced from the fact that the ordered fraction reaches 100% value at low temperature. In contrast, the asymmetry in Bi–Ca displays only a very slight deviation from its initial value below ≈170 K (figure 4(a)), thus evidencing that just a small fraction of the sample presents magnetic ordering (figure 5). This implies that the weak long-range magnetic order detected by neutrons comes from small minority regions in the sample. The second transition in the Bi–Ca compound must be ascribed to the development of a magnetic transition below 70 K in less than 30% of the Bi–Ca sample (figure 5). NPD data evidence that this transition does not give rise to any magnetic diffraction peak and that it must be of short-range kind. In fact, NPD data evidence an enhancement of the small-angle background intensity below this temperature (see the inset in figure 2(b)). It is important to recall that the Bi–Ca compound

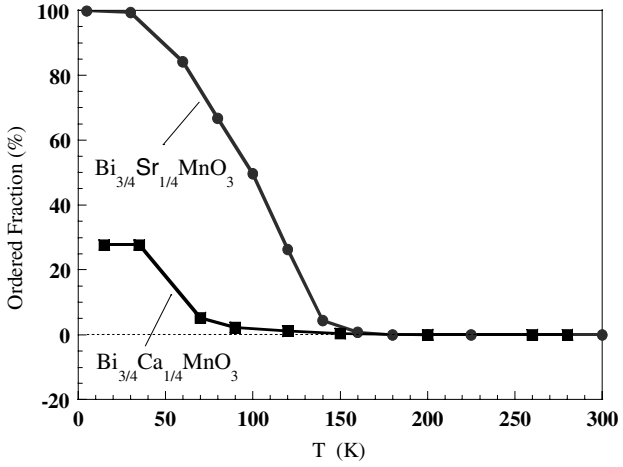

Figure 5. Comparison of the thermal dependence of the fraction of muons sensing a local static magnetic field in $Bi_{3/4}A_{1/4}MnO_3$ with A = Sr and Ca.

exhibits exponential relaxation ($\beta = 1$) above 170 K but below this temperature β decreases and deviates from 1 (see the inset of figure 4(b)) signalling the appearance of inhomogeneous magnetism in this compound. Therefore, a remarkable finding is the absence of long-range magnetic order in the majority regions of $Bi_{3/4}Ca_{1/4}MnO_3$.

4. Summary and conclusions

The magnetic and electronic properties of $Bi_{3/4}Ca_{1/4}MnO_3$ have been investigated in comparison with $Bi_{3/4}Sr_{1/4}MnO_3$. We have found that the differences between the two families of compounds (Ca and Sr doping) previously reported for $x = 0.50$ [1–3] do not diminish on reducing the doping level to $x = 1/4$. Diffraction and μSR data confirm different structural magnetic and electronic transitions in the manganites with commensurate charge balance $Bi_{0.75}Sr_{0.25}MnO_3$ and $Bi_{0.75}Ca_{0.25}MnO_3$. The study reveals that the dissimilarities between the two systems are greater than in the half-doped case.

The ground state of both compounds present charge and/or orbital order characterized by the appearance of new superstructure peaks that can be indexed on the basis of a $2a \times b \times 2c$ supercell. But the evolution of cell parameters evidences different electronic transitions at different temperatures. The Ca compound presents an anisotropic cell change between 200 and 300 K, above which, the cell parameters behave smoothly in all the studied temperature range. In contrast, the Sr compound presents a structural transition at a much higher temperature (600 K). Moreover, the evolution of cell parameters across these transitions is markedly different: in the Sr case a strongly increases (on cooling) and c and b shrink, while in the Ca case b contracts on cooling, and a and c are weakly lengthened at the transition. Furthermore, their magnetic properties strongly differ. The unexpected magnetic behaviour of $Bi_{0.75}Ca_{0.25}MnO_3$ requires a charge and orbital order distinct to that in $Bi_{0.75}Sr_{0.25}MnO_3$. Long-range antiferromagnetic order was found in $Bi_{0.75}Sr_{0.25}MnO_3$ [9] (a canted structure appears under applied field). This contrasts with the Ca results from NPD and μSR data. The low-temperature state presents short-range magnetism and spin disorder. A very significant fraction of the system ($\approx$70%) does not present local magnetic order. An inhomogeneous magnetic state has been detected below $\approx$150 K, coinciding with the appearance of a very weak

residual signature of minority regions with pseudo-CE-type order. Under zero field the two compositions investigated do not show a ferromagnetic component, ruling out the appearance of spontaneous ferromagnetism. However, the application of magnetic fields produces a continuous progressive canting of the moments, clearly visible even for relatively small fields.

Acknowledgments

Financial support by the Spanish Ministry of Education and Science (MAT2003-07483-C02-02 and MAT2006-11080-C02-02) and Generalitat de Catalunya (2005-GRQ-00509) is appreciated. We thank X G Capdevila for his help during sample preparation. We thank ISIS, the Institute Laue-Langevin, the CRG-D1B and the European Synchrotron Radiation Facility for the provision of beam time. The European Commission (HPRI, NMI3 and Access to ISIS Muons programmes) and the Functionalized Advanced Materials and Engineering European Network of Excellence are also acknowledged.

References

[1] Frontera C, García-Muñoz J L, Llobet A, Ritter C, Alonso J A and Rodríguez-Cavajal J 2000 *Phys. Rev.* B **62** 3002
[2] García-Muñoz J L, Frontera C, García-Aranda M A, Llobet A and Ritter C 2001 *Phys. Rev.* B **63** 064415
[3] Hervieu M, Maignan A, Martin C, Nguyen N and Raveau B 2001 *Chem. Mater.* **13** 1356
[4] Beran P, Malo S, Martin C, Maignan A, Nevrîva M, Hervieu M and Raveau B 2002 *Solid State Sci.* **4** 917
[5] Frontera C, García-Muñoz J L, Ritter C, Mañosa L, Capdevila X and Calleja A 2003 *Solid State Commun.* **125** 277
García-Muñoz J L, Frontera C, Aranda M A G, Ritter C, Llobet A, Respaud M, Goiran M, Rakoto H, Masson O, Vanacken J and Broto J M 2003 *J. Solid State Chem.* **171** 84
[6] Hervieu M, Malo S, Perez O, Beran P, Martin C and Raveau B 2003 *Chem. Mater.* **15** 523
[7] Frontera C, García-Muñoz J L, Hervieu M, Aranda M A G, Ritter C, Mañosa Ll, Capdevila X G and Calleja A 2003 *Phys. Rev.* B **68** 0134408
[8] Mantytskaya O S, Troyanchuk I O and Chobot A N 2004 *Low Temp. Phys.* **30** 218
[9] García-Muñoz J L, Frontera C, Respaud M, Giot M, Ritter C and Capdevila X G 2005 *Phys. Rev.* B **72** 054432
[10] Subías G, García J, Beran P, Nevřiva M, Sánchez M C and García-Muñoz J L 2006 *Phys. Rev.* B **73** 205107
[11] Seshadri R and Hill N A 2001 *Chem. Mater.* **13** 2892
[12] Kimura T, Kawamoto S, Yamada I, Azuma M, Takano M and Tokura Y 2003 *Phys. Rev.* B **67** 180401(R)
[13] Moreira dos Santos A, Parashar S, Raju A R, Zhao Y S, Cheetham A K and Rao C N R 2002 *Solid State Commun.* **122** 49
[14] Chiba H, Atou T and Syono Y 1997 *J. Solid State Chem.* **132** 139
[15] García-Muñoz J L, Frontera C, Hervieu M, Giot M, Respaud M, Calleja A and Capdevila X G 2006 *Bol. Soc. Esp. Ceram.* V **45** 233–7
[16] Goff R J and Attfield J P 2006 *J. Solid State Chem.* **179** 1369
[17] Cox D E, Radaelli P G, Marezio M and Cheong S-W 1999 *Phys. Rev.* B **57** 3305
[18] Atou T, Chiba H, Ohoyama K, Yamaguchi Y and Syono Y 1999 *J. Solid State Chem.* **145** 639
[19] Giot M, Pautrat A, Perez O, Simon C, Nevriva M and Hervieu M 2006 *Solid State Sci.* **8** 1414
[20] Montanari E, Righi L, Calestani G, Migliori A, Gilioli E and Bolzoni F 2005 *Chem. Mater.* **17** 1765
[21] Kirste A, Goiran M, Respaud M, Vanacken J, Broto J M, Rakoto H, von Ortenberg M, Frontera C and García-Muñoz J L 2003 *Phys. Rev.* B **67** 134413
[22] Respaud M, Llobet A, Frontera C, Ritter C, Broto J M, Rakoto H, Goiranand M and García-Muñoz J L 2000 *Phys. Rev.* B **61** 9014–8